

Discrete-Symmetry Breaking and Novel Critical Phenomena in an Antiferromagnetic Planar (XY) Model in Two Dimensions

D. H. Lee, J. D. Joannopoulos, and J. W. Negele

Department of Physics, Massachusetts Institute of Technology, Cambridge, Massachusetts 02139

and

D. P. Landau

Department of Physics, University of Georgia, Athens, Georgia 30602

(Received 14 November 1983)

Landau-Ginzburg-Wilson symmetry analyses and Monte Carlo calculations for the classical antiferromagnetic planar (XY) model on a triangular lattice reveal a wealth of interesting critical phenomena. From this simple model arise a zero-field transition to a state of long-range order, a new mechanism for spin disordering, and a critical point associated with a possible new universality class.

PACS numbers: 64.60.Cn, 05.70.Fh, 05.70.Jk, 75.10.Ak

Two-dimensional spin systems cannot exhibit long-range order by breaking a continuous symmetry at finite temperature.¹ Although order-disorder transitions are thereby excluded, Kosterlitz and Thouless (KT)² showed that the classical two-dimensional ferromagnetic planar (XY) model exhibits a unique phase transition from an algebraically ordered phase to a disordered phase via the unbinding of vortex pairs. Whereas the antiferromagnetic planar model on a bipartite (e.g., square) lattice is equivalent to the ferromagnetic model, the antiferromagnetic case for a tripartite (e.g., triangular) lattice is fundamentally different because of the inherent frustration.³ In this work, we use Landau-Ginzburg-Wilson (LGW) symmetry analyses and Monte Carlo (MC) calculations to study the phases of the antiferromagnetic planar (AFP) model, $\mathcal{H} = J \sum_{\langle ij \rangle} (s_i^x s_j^x + s_i^y s_j^y)$, on a triangular and a square lattice and find dramatic differences in their critical behavior and underlying physics.

An essential feature distinguishing the triangular and bipartite AFP models is the existence of discrete as well as continuous degeneracy in the triangular AFP ground state. For a bipartite lattice, a ground state consists of spins on two sublattices aligned in opposite directions. For the triangular lattice, a ground state consists of spins on three sublattices forming $\pm 120^\circ$ angles leading to a $\sqrt{3} \times \sqrt{3}$ periodicity. In a bipartite lattice global spin rotation generates all possible ground states, while an extra lattice reflection is needed for the triangular lattice. In Fig. 1, we show two ground states of the triangular lattice which are not obtainable from each other by global spin rotation. This additional symmetry breaking is manifested by the opposite helicity⁴

ordering of the two ground states. As a consequence, the system supports solitons (domain walls) as additional elementary excitations. An example of a soliton is shown in Fig. 1.

The order parameter associated with the $\sqrt{3} \times \sqrt{3}$ periodicity is given by $|\vec{\psi}|$, where the complex vector $\vec{\psi}$ is defined as

$$\vec{\psi} = \begin{pmatrix} \psi_{\parallel} \\ \psi_{\perp} \end{pmatrix} \equiv \frac{1}{N} \sum_{i=1}^N \exp(-i\vec{q} \cdot \vec{R}_i) \vec{s}_i. \quad (1)$$

Here $q = (\pm \frac{4}{3}\pi, 0)$ and $\psi_{\parallel}, \psi_{\perp}$ are orthogonal components of $\vec{\psi}$ chosen parallel and perpendicular to the magnetic field when $H \neq 0$. In terms of $\vec{\psi}$, the staggered helicity⁴ is given by $\eta = \text{Re}(\vec{\psi}) \times \text{Im}(\vec{\psi}) \equiv |\psi|^2 \sin \varphi$. Since lattice reflection is a discrete symmetry, the system can have long-range helicity order without violating the Mermin-Wagner theorem.¹ The zero-field low-temperature phase is therefore characterized by $\langle \vec{\psi} \rangle = 0$ and $\langle \eta \rangle = \pm 1$ so that although both $\text{Re}(\vec{\psi})$ and $\text{Im}(\vec{\psi})$ have no long-range order, they are locked in phase (φ).

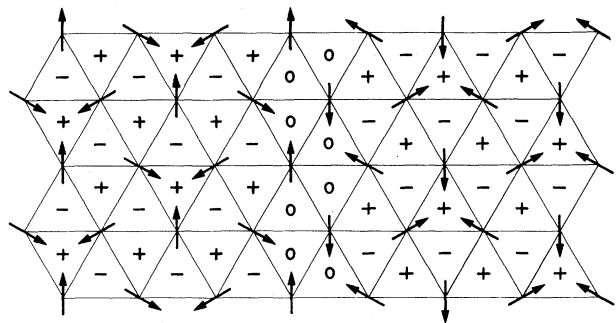


FIG. 1. Two ground states of opposite staggered helicity separated by a domain wall. The helicity of each triangle is indicated.

As the temperature increases, two spin-disordering mechanisms compete: the unbinding of the vortex pairs in both $\text{Re}(\bar{\psi})$ and $\text{Im}(\bar{\psi})$ and the unlocking of the phase correlation between $\text{Re}(\bar{\psi})$ and $\text{Im}(\bar{\psi})$. The latter process takes place through the creation of solitons and the transition occurs when the surface free energy associated with the soliton vanishes. Using simple stability arguments^{2,5} we find that the pair unbinding temperature T_v is roughly twice the temperature T_s associated with a soliton transition. This suggests that helicity order will be lost first, with a spontaneous generation of solitons. As verified by MC results shown below, the solitons screen the vortex interaction and induce pair unbinding immediately. This mechanism for spin disordering is fundamentally different from vortex pair unbinding and leads to what seems to be a new universality class of critical phenomena.

In the presence of an in-plane magnetic field the ground states still preserve the $\sqrt{3} \times \sqrt{3}$ periodicity. The sublattice ground-state magnetizations $\vec{m}_1, \vec{m}_2, \vec{m}_3$ satisfy $|\vec{m}_i| = 1$ for all i and

$$\sum_{i=1}^3 \vec{m}_i = \vec{H}/3J. \quad (2)$$

Surprisingly, even though the Hamiltonian has no continuous symmetry, there exist continuously degenerate solutions to (2). Moreover, it can be shown that at zero temperature as H is increased above $H_1 = 3J$, the solutions to (2) change from two disconnected manifolds (corresponding to two helicity states) to one manifold (corresponding to a state of zero helicity). Above $H_2 = 9J$ all the spins are aligned, leading to the paramagnetic phase.

The entire H - T phase diagrams for both square and triangular AFP models determined by MC calculations are shown in Fig. 2. (The simulations are performed with use of standard techniques⁶ for $L \times L$ lattices with periodic boundary conditions, with L up to 72. Data were obtained with use of between 2000 and 6000 MC steps for locating phase boundaries and as many as 4×10^4 MC steps for studying critical behavior.) The phase diagram for the square lattice (top panel) is easily understood. At $H = 0$, there is a conventional KT transition at $T_v = [0.90(2)]J$. At $H \neq 0$, only two degenerate ground states remain, leading to an Ising order-disorder phase boundary. For the triangular lattice (bottom panel) the phase diagram is far richer including four phase boundaries and three multicritical points T_s , H_1 , and A . The zero-field critical temperature T_s

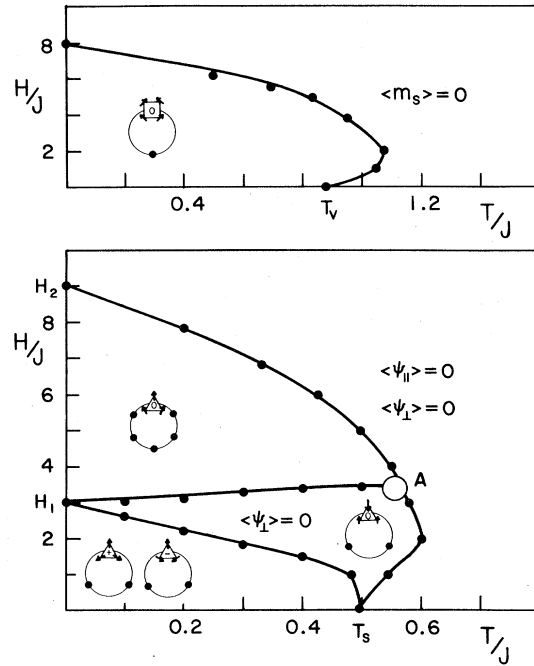


FIG. 2. Phase diagrams for AFP models on the square (top) and triangular (bottom) lattices. Components of the order parameters which are zero are indicated explicitly. The circle diagrams illustrate the spin configurations in the ordered phases. The dots around the circles represent the number of additional distinct and degenerate spin configurations obtained by permuting the sublattices. The manner in which the three phase boundaries merge at A is not determined precisely in this work.

$= [0.495(5)]J$ is associated with spontaneous generation of solitons as described earlier.

Since MC results indicate that all the phase boundaries shown in Fig. 2 are continuous transitions, LGW symmetry analyses were performed to understand their nature. All the invariants of the LGW Hamiltonian (to infinite order) can be built up from twelve elements. The first few terms in this expansion are

$$\mathcal{H}_{\text{LGW}} = \mathcal{H}(\psi_{\parallel}) + \mathcal{H}(\psi_{\perp}) + V(\psi_{\parallel}, \psi_{\perp}),$$

where

$$\mathcal{H}(\psi_{\parallel}) = \mathcal{H}_2(\psi_{\parallel}) + a\text{Re}(\psi_{\parallel}^3) + \dots,$$

$$\mathcal{H}(\psi_{\perp}) = \mathcal{H}'_2(\psi_{\perp}) + a'\text{Re}(\psi_{\perp}^6) + \dots,$$

$$V(\psi_{\parallel}, \psi_{\perp}) = b\text{Re}(\psi_{\parallel}\psi_{\perp}^2) + c\text{Re}[(\psi_{\parallel}\psi_{\perp}^*)^2] + d\text{Im}[(\psi_{\parallel}\psi_{\perp}^*)^2] + \dots \quad (3)$$

Here \mathcal{H}_2 and \mathcal{H}'_2 define isotropic two-component

Hamiltonians of the form

$$\mathcal{H}_2(\psi_{\parallel}) = r_2 |\psi_{\parallel}|^2 + r_4 |\psi_{\parallel}|^4 + r_6 |\psi_{\parallel}|^6 + \dots \quad (4)$$

In (3), $\mathcal{H}(\psi_{\parallel})$ and $\mathcal{H}(\psi_{\perp})$ describe three-state Potts⁷ and $Z(6)$ ⁸ models, respectively. This may be understood physically by noting that when the restriction $|\vec{s}_i|=1$ is neglected, at $H \neq 0$ the parallel or perpendicular components correspond to an antiferromagnetic triangular Ising model with or without an external field, respectively. Given (3), as the temperature decreases, the system can order via two alternative processes: (a) ψ_{\parallel} orders first, after which ψ_{\perp} can then order at a lower temperature. (b) ψ_{\perp} orders first and immediately orders ψ_{\parallel} by inducing an external field through the cubic term in $V(\psi_{\parallel}, \psi_{\perp})$. The universality classes of these transitions are analyzed as follows. For case (a), when ψ_{\parallel} becomes critical first, the transition belongs to the three-state Potts universality class. In the ordered phase two sublattices have spins pointing parallel to the field, while the other sublattice has spins pointing antiparallel to the field. The three Potts states correspond to the three alternative choices of the sublattice with antiparallel spins. The resulting LGW Hamiltonian for $\psi_{\perp} \equiv \sigma + i\tau$ is then

$$\begin{aligned} \mathcal{H}(\psi_{\perp}) &\equiv \mathcal{H}(\psi_{\perp}) + V(\langle \psi_{\parallel} \rangle, \psi_{\perp}) \\ &= \bar{a}\sigma^2 + \bar{b}\tau^2 + \bar{c}\sigma^4 + \bar{d}\tau^4 + \bar{e}\sigma^2\tau^2 + \dots \end{aligned} \quad (5)$$

This Hamiltonian has the same symmetry as the Ashkin-Teller⁹ and asymmetric eight-vertex¹⁰ models. For case (b), in which ψ_{\perp} orders first, considering only $\mathcal{H}(\psi_{\perp})$ would indicate that the transition is of the $Z(6)$ universality class⁸ and may have an intermediate algebraic phase. However, since induced ψ_{\parallel} ordering may break the $Z(6)$ symmetry, the situation is more complicated

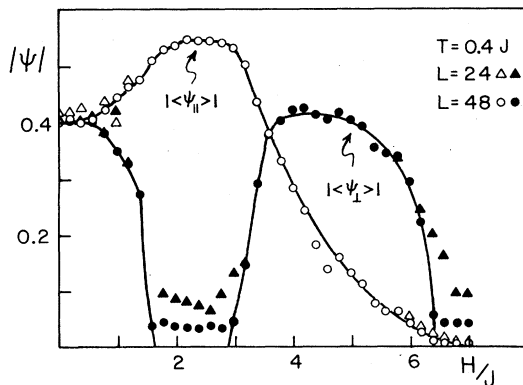


FIG. 3. Parallel and perpendicular components of the order parameter as a function of magnetic field.

and is currently under investigation.

The choice between cases (a) and (b) has been determined from MC calculations. In Fig. 3, we show the order parameters $|\langle \psi_{\parallel} \rangle|$ and $|\langle \psi_{\perp} \rangle|$ at $T=0.4J$ as functions of magnetic field. Two ordered phases with $|\langle \psi_{\parallel} \rangle| \neq 0$ and $|\langle \psi_{\perp} \rangle| \neq 0$ are separated by an intermediate phase with $|\langle \psi_{\parallel} \rangle| \neq 0$ but $|\langle \psi_{\perp} \rangle| = 0$. In Fig. 2, the intermediate phase corresponds to the region bounded by H_1, A, T_s , with the fully ordered phases corresponding to the regions above and below. These results indicate that along the phase boundary $A-T_s$, ψ_{\parallel} orders while ψ_{\perp} does not, thus realizing case (a). The three-state Potts phase inside the boundary is illustrated by the circle diagram representing the three possible spin configurations. Case (b) is realized along the phase boundary $A-H_2$, giving rise to the six spin configurations depicted by the circle diagram.

The remaining two inner phase boundaries of the triangular lattice in Fig. 2 correspond to the ordering of σ and τ . From Eq. (4) either σ , τ , or both σ and τ may order across these boundaries. MC calculations (not shown) indicate that σ orders at the upper boundary H_1-A while τ orders at the lower boundary H_1-T_s . The distinction between the upper and lower fully ordered phases is that the lower phase has nonzero helicity. The six possible states in the lower region are shown by the circle diagrams with positive and negative helicity.

Finally, the critical behavior at $H=0$ and $T=T_s$,

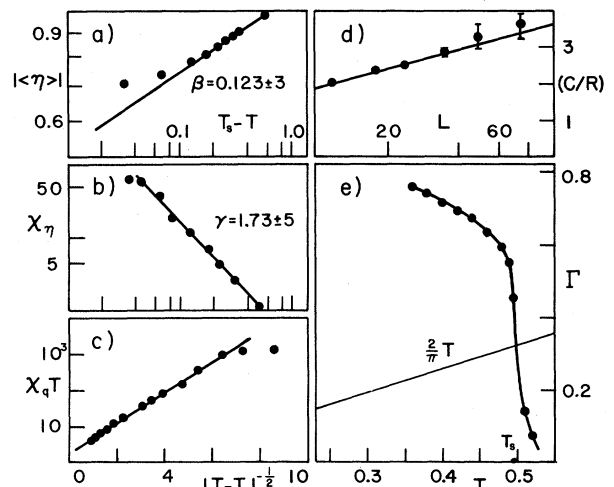


FIG. 4. Critical behavior at $H=0$ and $T=T_s$ for $J=1$. (a) Staggered helicity, (b) fluctuations in staggered helicity, (c) fluctuations in order parameter $\vec{\psi}$, (d) maximum specific heat, and (e) spin-helicity modulus.

has been studied in detail by MC with the results shown in Fig. 4. Considering finite-size effects and restricting ourselves to our best estimate of T_s , we find that the staggered helicity and its fluctuation have Ising-like critical exponents $\beta = 0.123(3)$ ($\frac{1}{8}$) and $\gamma = 1.73(5)$ ($\frac{7}{4}$), respectively. In contrast, the fluctuation of the staggered magnetization ($|\overline{\psi}|$) is consistent with the KT form¹ $\exp\{c[T - T_s]^{-1/2}\}$. The specific heat is dominated by the leading singularity, and seems to have Ising behavior as shown in Fig. 4(d). The spin-helicity modulus³ Γ , unlike that of the KT transition, seems to display a jump greater than the universal value of $(2/\pi)T_s$. These results, taken together, suggest that the transition at T_s may constitute a new universality class.

In summary, the essential physical results of this work are the following. An exceedingly simple model leads to a surprising richness of phases and critical behavior. The underlying triangular lattice and the associated degeneracy play a crucial role in this physics. A mechanism for long-range order has been demonstrated which does not violate the Mermin-Wagner theorem and a soliton has been introduced and shown to induce the $H=0$ phase transition.

It is a pleasure to acknowledge helpful discussions with A. N. Berker, D. Blankschtein, P. A. Lee, D. R. Nelson, S. Teitel, and F. Y. Wu. One of the authors (J.W.N.) gratefully acknowledges

fellowship support by the John Simon Guggenheim Memorial Foundation. This work was supported in part by U. S. Office of Naval Research Grant No. N00014-77-C-0132, National Science Foundation Grant No. DMR-8300754, and U. S. Department of Energy Contract No. BE-AC02-76ER03069.

¹N. D. Mermin and H. Wagner, Phys. Rev. Lett. **17**, 1133 (1966).

²J. M. Kosterlitz and D. J. Thouless, J. Phys. C **5**, 124 (1972), and **6**, 1181 (1973); J. M. Kosterlitz, J. Phys. C **7**, 1046 (1974).

³S. Teitel and C. Jayaprakash, Phys. Rev. B **27**, 598 (1983).

⁴The helicity for each triangle is defined as $\Sigma \Delta\theta/2\pi$, where $\Delta\theta$ is the smallest clockwise change in angle when each triangle is traversed in a clockwise fashion. Only +1, -1, and 0 values of helicity are possible for any given triangle. A staggered-helicity order parameter may be defined as the sum of helicity over all triangles with alternating signs for adjacent triangles.

⁵E. Müller-Hartmann and J. Zittartz, Z. Phys. B **27**, 261 (1977).

⁶K. Binder and D. P. Landau, Phys. Rev. B **13**, 1140 (1976).

⁷F. Y. Wu, Rev. Mod. Phys. **54**, 235 (1982).

⁸J. V. Jose, L. P. Kadanoff, S. Kirkpatrick, and D. R. Nelson, Phys. Rev. B **16**, 1217 (1977).

⁹J. Ashkin and E. Teller, Phys. Rev. **64**, 178 (1943).

¹⁰R. J. Baxter, Phys. Rev. Lett. **26**, 832 (1971).